

Bidirectional electric communication between the inferior occipital gyrus and the amygdala during face processing

Running head: IOG–amygdala coupling during face processing

Wataru Sato^{1,†}, Takanori Kochiyama^{2,†}, Shota Uono¹, Kazumi Matsuda³, Keiko Usui³, Naotaka Usui³, Yushi Inoue³, and Motomi Toichi⁴

¹ Department of Neurodevelopmental Psychiatry, Habilitation and Rehabilitation, Graduate School of Medicine, Kyoto University. ² Brain Activity Imaging Center, Advanced Telecommunications Research Institute International. ³ National Epilepsy Center, Shizuoka Institute of Epilepsy and Neurological Disorders. ⁴ Faculty of Human Health Science, Graduate School of Medicine, Kyoto University. † Equal contributors.

Corresponding author: Wataru Sato. Department of Neurodevelopmental Psychiatry, Habilitation and Rehabilitation, Graduate School of Medicine, Kyoto University, 53 Shogoin-Kawaharacho, Sakyo, Kyoto 606-8507, Japan. E-mail: sato.wataru.4v@kyoto-u.ac.jp

Abstract

Faces contain multifaceted information that is important human communication. Neuroimaging studies have revealed face-specific activation in multiple brain regions, including the inferior occipital gyrus (IOG) and amygdala; it is often assumed that these regions constitute the neural network responsible for the processing of faces. However, it remains unknown whether and how these brain regions transmit information during face processing. This study investigated these questions by applying dynamic causal modeling of induced responses to human intracranial electroencephalography data recorded from the IOG and amygdala during the observation of faces, mosaics, and houses in upright and inverted orientations. Model comparisons assessing the experimental effects of upright faces vs. upright houses and upright faces vs. upright mosaics consistently indicated that the model having face-specific bidirectional modulatory effects between the IOG and amygdala was the most probable. The experimental effect between upright vs. inverted faces also favored the model with bidirectional modulatory effects between the IOG and amygdala. The spectral profiles of modulatory effects revealed both same- (e.g., gamma–gamma) and cross- (e.g., theta–gamma) frequency couplings. These results suggest that the IOG and amygdala communicate rapidly with each other using various types of oscillations for the efficient processing of faces.

Keywords: amygdala; cross-frequency coupling; dynamic causal modeling (DCM); face; gamma oscillation; inferior occipital gyrus; intracranial electroencephalography (EEG).

INTRODUCTION

Faces convey information that is important for social interactions in humans. Behavioral researchers have pointed out that faces are unique among visual objects, because they are socially relevant and contain multifaceted information, including cues pertaining to emotional content or one's identity [Ekman and Friesen, 1975; Bruce and Young, 1986]. Behavioral studies empirically confirmed that faces are perceived more rapidly [Purcell and Stewart, 1986; Ro et al., 2001; Hershler and Hochstein, 2005; Tottenham et al., 2006; Landau and Bentin, 2008] and memorized more accurately [Yin, 1969, 1970; Sato and Yoshikawa, 2013] than other objects. The studies also showed that multifaceted information in faces is processed in an integrative manner that supports such efficient/robust face processing [McKelvie, 1995; Calder et al., 2000; Öhman et al., 2001; Milders et al., 2006; Sato and Yoshikawa, 2010]. Furthermore, the visual processing of faces may be distinct in that faces are processed based on configurations as well as features, whereas objects are mainly processed based on features [e.g., Young et al., 1987; Tanaka and Farah, 1993; for a review, see Tanaka and Simonyi, 2016].

Several functional neuroimaging studies using magnetic resonance imaging (MRI) and positron emission tomography have explored the neural mechanisms involved in face processing and have revealed that the observation of faces induces heightened hemodynamic responses in multiple specific brain regions, including neocortical visual areas, such as the inferior occipital gyrus (IOG), and limbic regions, such as the amygdala [e.g., Blonder et al., 2004; Gauthier et al., 2000; Ishai et al., 2005; Rossion et al., 2012]. Studies further suggested that these face-responsive regions serve different functions. For example, the IOG was reported to be active during the visual analysis of features [Liu et al., 2010a] and configurations [Rossion et al., 2011] of faces, whereas activity in the amygdala reportedly changed depending on the emotional significance of faces (faces elicit negative emotions or not) irrespective of their low-level visual properties [Sato et al., 2004]. Anatomical MRI studies using diffusion tensor imaging revealed that the IOG and amygdala exhibit white-matter connections that receive visual input via the optic radiation–occipital early visual cortices [Gschwind et al., 2012] and the superior colliculus–pulvinar [Rafal et al., 2015; Tamietto et al., 2012], respectively. These data suggest that both of these regions are capable of rapid and independent face processing. At the same time, postmortem [Latini, 2015] and anatomical MRI [Catani et al., 2003] studies have suggested that the occipital cortices including the IOG and the anterior temporal cortices close to the amygdala have direct white-matter connectivity, implying that these regions may constitute a functional network. This notion is in line with the view that the cortical and subcortical face-responsive regions constitute a widespread neural network [Haxby et al., 2000]. The possible communication among these brain regions may explain the behavioral evidence of integrated processing of multifaceted face-related information.

However, it remains unclear whether the IOG and amygdala constitute a functional neural network underlying the processing of faces. A previous functional MRI study has failed to find clear evidence supporting the functional coupling of the IOG and amygdala during face processing [Davies-Thompson and Andrews, 2012]. However, this result may have been due to the technical limitations associated with measuring hemodynamic responses with functional MRI, because this is an indirect

measure of neural activity and lacks the temporal resolution needed to accurately depict neuronal firing [cf. Mukamel and Fried, 2012].

By contrast, intracranial electroencephalography (EEG) can provide direct electric information regarding neural activity with good temporal and spatial resolutions. Previous intracranial EEG studies have confirmed that the IOG and amygdala exhibit rapid activation during the observation of faces [Allison et al., 1999; Rosburg et al., 2010; Jonas et al., 2012; Sato et al., 2012, 2014]. The rapid interaction between these brain regions may underlie the behavioral advantages associated with the processing of faces relative to other objects. However, no studies have explored the electric communication between these regions during the processing of faces.

The present study investigated whether electric field potential activity between the IOG and amygdala would be indicative of communication during face processing, and if so, what the nature of this communication may be. To achieve these goals, we re-analyzed intracranial EEG data recorded from six participants undergoing pre-neurosurgical assessment during the presentation of faces, mosaics, and houses in upright and inverted orientations. In previous studies [Sato et al., 2012, 2014], we demonstrated that during the processing of faces, these regions exhibited gamma-band activity (higher than 30 Hz [Adrian, 1942]), which has been shown to correspond to hemodynamic responses [Foucher et al., 2003; Logothetis et al., 2001] and to be relevant for neural computation [e.g., Tallon-Baudry et al., 1996; for a review, see Herrmann et al., 2010]. In the amygdala, face-related gamma-band activation was evident in the lateral part, which is consistent with previous findings showing that the laterobasal subregion of the amygdala is involved in social functions in monkeys [Nakamura et al., 1992; Gothard et al., 2007] and humans [Hurlmann et al., 2008; Sato et al., 2016]. Lower-frequency activity was also evident during the observation of faces in the IOG. In addition, we found that the inverted presentation of faces, which impairs configural/holistic visual processing of faces [e.g., Sergent, 1984; Farah et al., 1995; for a review, see Civile et al., 2014], modulated gamma-band activity in the IOG. We further found that the presentation of faces modulated the cross-frequency coupling in the IOG between theta and gamma oscillations, which has been argued to be an indication of communication among neural populations [e.g., Liebe et al., 2012; for reviews, see von Stein and Sarnthein, 2000; Canolty and Knight, 2010].

In the present study, we analyzed the intracranial EEG data using dynamic causal modeling (DCM) of induced responses [Chen et al., 2008]. DCM allows the investigation of effective connectivity, that is, the causal and directional influences between one brain region and another [Friston et al., 2003]. Although DCM was originally proposed as the analytic tool for functional MRI data [Friston et al., 2003], the DCM of induced responses was extended to analyze the time-varying power spectra of electrophysiological signals [Chen et al., 2008]. Previous studies have successfully applied DCM of induced responses to scalp-recorded EEG [Chen et al., 2008] and magnetoencephalography (MEG) [Furl et al., 2014]] data to reveal the neocortical networks underlying face processing. In DCM, researchers generally construct hypothesized and alternative models and then identify the most appropriate model through model selection. In our models, we assumed that the IOG and amygdala have bidirectional intrinsic (i.e., baseline) connectivity based on the anatomical evidence [Catani et al., 2003; Latini, 2015]. Then, we tested whether unidirectional or

bidirectional connections were likely to modulate the effects of face (upright face vs. upright house and upright face vs. upright mosaic) and face inversion (upright face superiority; upright face vs. inverted face). We also tested modulations of self or recurrent connections [Friston et al., 2003] to confirm the intra-regional coupling previously reported for the IOG [Sato et al., 2014]. Based on the behavioral data showing integration of multifaceted information during face processing [e.g., Öhman et al., 2001], we predicted that the optimal model would be one with face-induced and face-inversion-induced bidirectional modulatory effects between the IOG and amygdala.

Furthermore, because the DCM of induced responses [Chen et al., 2008] allowed us to investigate the spectral profile of connections by showing amplitude–amplitude same- and cross-frequency couplings [cf. Canolty and Knight, 2010], we hoped to specify the frequency patterns of intra- and inter-regional modulatory effects. Previous studies have reported that DCM of induced responses revealed the spectral profiles of same- and cross-frequency couplings among neocortical regions during face processing [Chen et al., 2008; Furl et al., 2014]. Based on previous intracranial EEG data showing the gamma-band activity and intra-regional theta–gamma cross-frequency coupling related to face processing in the IOG [Sato et al., 2014], together with ample evidence of same-frequency gamma-band couplings [e.g., Rodriguez et al., 1999; for a review, see Varela et al., 2001], we predicted that the intra- and inter-regional communication among the IOG and amygdala would utilize same- and cross-frequency couplings related to the gamma band.

METHODS

Participants

This study included six patients (five females, one male; mean \pm SD age: 34.5 ± 7.9 years) suffering from pharmacologically intractable focal epilepsy. The background demographics and clinical information of the patients is summarized in Table 1. Intracranial electrodes were implanted in the patients during the course of pre-surgical evaluation, and electrophysiological and surgical examination revealed that the main epileptic foci were in the hippocampi of five participants and in the anterior lateral temporal cortex of one participant. The experiment was conducted 2.0–2.8 weeks after electrode implantation. None of the patients showed any neurological or psychiatric problems other than those associated with epilepsy. All patients were taking antiepileptic medications and were mentally stable at the time of the experiments. During the experiments, no seizure activity was observed. All patients were right-handed as assessed by the Edinburgh Handedness Inventory [Oldfield, 1971], possessed normal or corrected-to-normal visual acuity, and provided written informed consent following a full explanation of the procedure. This study was approved by the local institutional ethics committee.

Anatomical assessment

Pre- and post-implantation anatomical assessments were conducted using structural MRI with a 1.5-T scanning system (Signa TwinSpeed, General Electric Yokokawa) and T-1 weighted images. Three-dimensional fast spoiled gradient-recalled acquisition was performed using the following parameters: repetition time = 12 ms, echo time = 5 ms, flip angle = 20° , matrix size = 256×256 , field of view = 22×22 cm, and number of slices = 76, which resulted in voxel dimensions of $0.8594 \times 0.8594 \times 2.0$ mm thick. The pre-implantation MRI assessment and surgical evaluation of the

participants did not reveal any structural abnormalities in the bilateral IOG or the amygdala of any of the participants.

The implantation of intracranial electrodes was performed using the stereotactic method [Mihara and Baba, 2001], with implantation sites chosen solely based on clinical criteria. Subdural electrodes were implanted in the usual manner in both hemispheres of five participants and in the right hemisphere of one participant.

The electrodes of interest in the IOG and amygdala were selected based on anatomical and functional criteria. Our analyses were restricted to the right hemisphere, because (1) all participants had electrodes placed in both the IOG and amygdala in the right hemisphere, but not necessarily the left, and (2) face-related event-related potentials and gamma-band activities have been observed only in the right IOG [Sato et al., 2014]. Following implantation, an anatomical MRI assessment was conducted using MRICron software (<http://www.mccauslandcenter.sc.edu/mricro/mricron/>). This anatomical assessment confirmed that the third electrode (numbered in ascending order from the medial to the lateral side) was placed in the lateral part of the right amygdala in all participants (Fig. 1). Although the present electrode implantation procedure could not provide information regarding the locations of amygdala nuclei, our assessment using a probabilistic cytoarchitectonic map derived from human postmortem brain data [Amunts et al., 2005; Eickhoff et al., 2005] suggested that the mean electrode coordinates were located in the laterobasal subregion with a high probability (80%). Our assessment revealed two candidate electrodes for the IOG in all participants. We subsequently selected a single electrode for the IOG for each participant, choosing the one that showed a greater amplitude in response to faces vs. mosaics during the 100–200 ms interval following stimulus presentation.

Stimuli

Face stimuli were created using grayscale photographs (Fig. 2) and consisted of images of the full-face neutral expressions of seven female and seven male Japanese models. These stimuli were selected from our database of more than 50 Japanese models. The stimuli were 200×200 pixels in size. The mosaic stimuli were constructed by dividing all face stimuli into 625 squares comprising 8×8 pixels and randomly reordering the squares using a constant algorithm, which resulted in images that were unrecognizable as faces. The house stimuli consisted of grayscale photographs of 14 houses that were the same size as the face stimuli. In the inverted condition, all of the photographs were presented upside down. The mean luminance was held constant across all images using MATLAB 6.5 (Mathworks).

Procedure

The presentation of the stimuli was controlled by SuperLab Pro 2.0 (Cedrus), implemented on a Windows computer (FSA600, Teknos), and presented on a 19-inch CRT monitor (GDM-F400, Sony) with a refresh rate of 100 Hz and a resolution of 1024×768 pixels. The stimuli subtended a visual angle of $7.6^\circ \times 7.6^\circ$. The responses of participants were recorded using a response box (RB-400, Cedrus).

Experiments were conducted individually in a quiet room. Each participant seated comfortably 0.57 m from the monitor with her/his head supported by a chin-and-forehead rest.

Each stimulus was presented twice, and a red cross was presented as the target in 20 trials, which resulted in a total of 188 trials for each participant (28 trials each for the upright face, upright mosaic,

upright house, inverted face, inverted mosaic, and inverted house stimuli as well as 20 target trials). The stimuli were presented in random order. In each non-target trial, the stimulus was presented centrally for 1,000 ms after a small black cross ($0.5^\circ \times 0.5^\circ$) appeared at a fixation point for 500 ms. In each target trial, a larger red cross ($1.2^\circ \times 1.2^\circ$) was presented instead of the photo stimulus until the participants responded. Participants were asked to detect a red cross and press a button with their right forefinger as quickly as possible upon seeing the target stimulus. This dummy task ensured that participants were attending to the stimuli but did not require the controlled cognitive, emotional, or behavioral processing of the stimuli. Performance on the dummy target-detection task was perfect (correct identification rate = 100.0%; mean \pm SD reaction times: 403.1 ± 28.8 ms). Participants were also instructed not to blink while the stimuli were presented. The inter-trial interval varied randomly between 2,000 and 5,000 ms. To avoid habituation and drowsiness, participants were given a short rest upon completion of 25% of the trials. Prior to data collection, the participants were familiarized with the procedure by completing a training block of 10 trials.

Data recording

The recording of intracranial EEG data from the neocortical regions, including the IOG, was conducted using subdural platinum electrodes (2.3 mm diameter; Ad-tech) while the recording of data from the subcortical regions, including the amygdala, was conducted using depth platinum electrodes (0.8 mm diameter; Unique Medical). These electrodes were referenced to electrodes (2.3 mm diameter; Ad-tech) embedded inside the scalp of the midline dorsal frontal region. Impedances were balanced and maintained below 5 k Ω . Data were amplified, filtered online (band pass: 0.5–300 Hz), and sampled at 1,000 Hz onto the hard disk drive of the intracranial EEG system (EEG-1100; Nihon Kohden) while the online monitoring was conducted using a more restricted bandwidth of 0.5–120 Hz. Vertical and horizontal electrooculograms (EOGs) were simultaneously recorded using Ag/AgCl electrodes (Nihon Kohden). As in previous studies [Lachaux et al., 2003], off-line visual inspections confirmed that there was no contamination of the EOGs. Unobtrusive video recordings of the events were made using a video camera built into the intracranial EEG system, and an off-line analysis of the videos confirmed that all participants were fully engaged in the task.

Data analysis: preprocessing

All preprocessing was performed using the statistical parametric mapping package SPM8 (<http://www.fil.ion.ucl.ac.uk/spm>) implemented in MATLAB R2012b (Mathworks), which followed the same procedures in our previous study [Sato et al., 2014].

Data obtained over a 3,000 ms interval were sampled for each trial; pre-stimulus baseline data were collected for 1,000 ms and experimental data were collected for 2,000 ms after stimulus onset at a sampling rate of 1,000 Hz. Epochs containing signals for which the amplitude was $> \pm 800$ μ V were initially excluded, and subsequently, any epoch with an absolute signal amplitude value > 5 SD from the mean or median signal amplitude for each electrode for each participant was rejected as an artifact. The frequencies of artifact-contaminated trials did not differ across any of the conditions (upright face, upright mosaic, upright house, inverted face, inverted mosaic, or inverted house) for either hemisphere (mean \pm SD = $5.1 \pm 1.7\%$ and $5.2 \pm 2.1\%$ for the right and left IOG electrodes, respectively; $p > 0.45$, two-way repeated-measures analysis of variance). The observed time frequency maps were calculated for each trial using continuous wavelet decomposition with 7-cycle Morlet wavelets. Then, the maps were log-transformed and baseline-corrected with respect to mean power over the 250 ms pre-stimulus period separately for each frequency.

Data analysis: DCM of induced responses

To explore the effective connectivity between the IOG and amygdala, DCM of induced responses [Chen et al., 2008] was performed for IOG and amygdala intracranial EEG activity using SPM12, revision 6225. DCM generally allows one to draw inferences about the influences that one neural system has on another and how this is affected by the experimental context [Friston et al., 2003]. This variant of DCM models the time-varying power spectra of electrophysiological signals over a distributed source and a range of frequencies [Chen et al., 2008]. Using this analysis, we can examine the architectural and time-frequency properties of neural networks.

The DCM of induced responses employs the generative model, which represents how the measured time–frequency power responses are generated through amplitude–amplitude same- and cross-frequency couplings within the distributed neuronal network. Mathematically, the model treats electromagnetic spectral states as perturbations from their expected levels using the following differential equation:

$$\dot{g} = (A + vB)g + Cu,$$

where the change in the frequency-specific power at a source area is expressed as a function of power in all frequencies and connected areas. In the equation, g is time–frequency spectral responses that are concatenated across all regions. A is a matrix of intrinsic coupling parameters that encode changes in spectral responses induced by other sources. B is a matrix of modulatory coupling parameters that encode the modulation of the intrinsic coupling parameters in A by experimental effects v (e.g., experimental conditions or trial-types under which the responses are elicited). Matrix C represents the driving input on particular frequencies and regions as induced by exogenous (e.g., sensory stimulus) inputs u . The Bayesian inversion of the generative model allows for comparisons of different structural models or hypotheses about the network architecture based on the model evidence and enables inferences about the coupling parameters (i.e., the same- and cross-frequency couplings) of the best network model.

The preprocessed and epoched data were entered into a standard DCM processing stream [Chen et al., 2008, 2009, 2012; Litvak et al., 2011; Furl et al., 2015]. For computational expediency, the data were first downsampled to 250 Hz. The time–frequency spectra were then calculated for each trial using continuous wavelet decomposition with 5-cycle Morlet wavelets from 4 to 100 Hz in 1 Hz steps, which covered theta (4–8 Hz), alpha (8–12 Hz), beta (12–30 Hz), and gamma (30–100 Hz) activities. The time-window was set to 1–500 ms (note that a time window with an additional ± 512 ms was used during computation to avoid edge effects of the wavelet transform). The spectral magnitudes of the time–frequency responses were averaged to yield the induced response and then baseline-corrected with respect to mean power over one-eighth of the post-stimulus time bin (i.e. 60 ms) using the SPM default setting.

DCM allows for the modeling of three different types of interactions in a neural network: (1) the driving input, which embodies the influences of an exogenous input on neural states; (2) intrinsic connections, which represent baseline connectivity (i.e., applicable to all experimental conditions) among neural states; and (3) the modulation of intrinsic connections by experimental manipulations. The network models considered in this study are shown in Fig. 3. In all models, the driving input of visual stimulation was set to both the IOG and amygdala. The prior stimulus onset time was set at 64 ms with a dispersion of 16 (SPM defaults). Bidirectional intrinsic connections between the IOG and amygdala were present in all models. The effects of face and face-inversion were modeled to reflect the modulatory effects of each of these bidirectional connections. To test our hypotheses, we

constructed a total of eight network architectures by systematically changing the locations of these modulatory effects (Fig. 3). These included models with modulatory effects on no connections at all (M1), on inter-regional connections alone (M2–4), on intra-regional connections alone (M5), and on both inter-regional and intra-regional connections (M6–8). In addition, models with unidirectional effects (M2–3 and M6–7) and those with bidirectional effects on inter-regional connections (M4 and M8) were included. Each model contained only one type of modulation (upright face vs. upright house, upright face vs. upright mosaic, or upright face vs. inverted face conditions). Note that we assumed linear (within-frequency) and nonlinear (between-frequency) couplings among all connections, because the induction of cross-frequency coupling phenomena is mediated by nonlinearities among connections [Chen et al., 2008].

To identify the optimal IOG–amygdala network model, we conducted random-effects Bayesian model selection analyses [Stephan et al., 2009]. We used exceedance probabilities as the evaluation measures, based on the belief that one particular model was more likely to be accurate than the other models given the group data [cf. Liu et al., 2010b; Seghier et al., 2011]. To confirm the consistency of the model selection among participants, additional individual analyses were conducted using the same procedure as the group analysis except for the use of a fixed-effects Bayesian model selection analysis.

Then the winning model in the group analysis was used to make inferences regarding the frequency patterns of the modulatory connections. The frequency–frequency modulatory coupling parameters from four connections (IOG recurrent, IOG-to-amygdala, amygdala-to-IOG, and amygdala recurrent) for the six participants were converted into 2D images and smoothed using a Gaussian kernel with a full-width half-maximum of 8 Hz to compensate for inter-subject variability [Chen et al., 2012]. These images were considered subject-specific summary statistics. Subsequently, random-effects general linear model analyses were performed using a standard summary statistics approach. We computed three full factorial models to evaluate same- and cross-frequency couplings with respect to the modulatory effects of face (upright face vs. upright house and upright face vs. upright mosaic conditions) and face inversion (upright face vs. inverted face conditions). Finally, 2D SPM{t} values were calculated for positive/excitatory and negative/inhibitory effects with respect to the same- and cross-frequency couplings of each of the modulatory connections respectively. Because information specifying the spectral regions of interest was scarce, significant effects were assessed for the entire spectral range with a height threshold of $p < 0.05$ (uncorrected). To reduce the likelihood of type I errors, only consistent effects across both face effect contrasts (upright face vs. upright house and upright face vs. upright mosaic) were evaluated.

RESULTS

DCM model comparison

DCM for induced responses was applied to the intracranial EEG data (Fig. 4a) to test network models with different modulatory connectivities between the IOG and amygdala (Fig. 3). Of the DCM models testing the modulatory effects of face (upright face vs. upright house conditions and upright face vs. upright mosaic conditions), the exceedance probabilities of the random-effects Bayesian model selection analysis indicated that the model with bidirectional modulatory connectivity was the most likely (Fig. 5a). Of the models testing the modulatory effects of face

inversion (upright face superiority; upright face vs. inverted face conditions), the same model was indicated as the most likely (Fig. 5a). Fig. 4b shows the predicted time–frequency responses generated by the winning model. As is evident, the key spectral properties of the actual observed time–frequency responses align with these predicted responses.

To confirm the consistency of the model selection among participants, additional Bayesian model selection analyses were conducted using individual data. The results revealed that the model with bidirectional modulatory connectivity was the most favored in all experimental effects in all individuals (Fig. 5b).

Spectral profiles of modulatory couplings

The spectral profiles of the modulatory couplings are shown in Fig. 6. Significant same- and cross-frequency modulatory couplings were observed for both of the face effects; i.e., upright face vs. upright mosaic (Fig. 6a) and upright face vs. upright house conditions (Fig. 6b). Intra-amygdala modulation included negative gamma–gamma same- and beta–gamma cross-frequency couplings (red box (1) in Fig. 6a/b). Intra-IOG modulation included a positive cross-frequency coupling in the theta/alpha/beta–gamma band (red box (2) in Fig. 6a/b). With respect to IOG–amygdala inter-regional modulation, the theta/alpha band in the IOG facilitated the cross-frequency gamma band in the amygdala (red box (3) in Fig. 6a/b). For amygdala–IOG inter-regional modulation, the gamma band in the amygdala inhibited the cross-frequency theta/alpha band (red box (4) in Fig. 6a/b) and the same-frequency gamma band in the IOG (red box (5) in Fig. 6a/b).

To analyze the face-inversion effect (upright face superiority effect), the upright face vs. inverted face conditions were compared (Fig. 6c) and several significant same- and cross-frequency modulatory couplings, some of which were consistent with the above face effect, were found. As with the face effect, intra-amygdala modulation included a negative gamma–gamma same-frequency coupling (red box (1) in Fig. 6c) and intra-IOG modulation included a positive cross-frequency coupling in the theta/alpha/beta–gamma band (red box (2) in Fig. 6c). For the amygdala–IOG inter-regional modulation, the gamma band in the amygdala inhibited the same-frequency gamma band in the IOG (red box (5) in Fig. 6c). By contrast, some inter-regional modulations found in the face effect, such as the IOG–amygdala theta/alpha–gamma cross-frequency coupling (red box (3) in Fig. 6a/b) and the amygdala–IOG gamma–theta/alpha cross-frequency coupling (red box (4) in Fig. 6a/b), were not evident in this comparison.

DISCUSSION

The results of our DCM model selection revealed that the model that best accounted for the intracranial EEG data included recurrent intra-regional modulation for face processing (both upright face vs. upright mosaic and upright face vs. upright house conditions) in the IOG and amygdala. Spectral profiles revealed that this intra-regional modulation included theta–gamma cross-frequency couplings. These results are consistent with previous findings showing that the IOG exhibit an intra-regional theta–gamma cross-frequency coupling during face processing, based on an analysis using

an algorithm that differed from DCM [Sato et al., 2014]. In addition, our results yielded the novel finding that an intra-regional gamma–gamma same-frequency coupling was involved in face processing in the amygdala. Our results from the DCM model selection and spectral profiles also revealed that these intra-regional IOG theta–gamma and amygdala gamma–gamma couplings were involved in the modulatory effects of upright faces relative to inverted faces, which suggests these couplings are involvement in the configural/holistic visual processing for faces [Civile et al., 2014]. These results are consistent with findings of previous studies involving humans and animals that reported the same- and cross-frequency couplings of theta and gamma bands during several different kinds of information processing [e.g., Canolty et al., 2006; Montgomery and Buzsaki, 2007; for reviews, see Varela et al., 2001; Lisman and Jensen, 2013]. Our data indicate that intra-regional cross- and same-frequency couplings are critically relevant to face processing in the IOG and amygdala.

As a result of obtaining more important data relevant to our first research question regarding whether the IOG and amygdala communicate during face processing, our DCM model selection revealed that the IOG and amygdala exhibit bidirectional inter-regional modulation for both the face (both upright face vs. upright mosaic and upright face vs. upright house conditions) and face inversion (upright face vs. inverted face conditions) effects. These results are inconsistent with those of a previous functional MRI study that reported a null result with regard to the functional connectivity between the IOG and amygdala during face processing [Davies-Thompson and Andrews, 2012]. However, these discrepant results may be explained by methodological differences; the intracranial EEG method, unlike functional MRI, can directly record electrical field potential activity at a high temporal resolution [cf. Mukamel and Fried, 2012]. Moreover, our current results are consistent with anatomical evidence that the IOG and amygdala have direct white-matter connections in humans [Catani et al., 2003; Latini, 2015]. Our MRI assessment using the probabilistic cytoarchitectonic map suggested that our amygdala electrodes were located at the laterobasal subregion, and this is in line with anatomical evidence in monkeys that the laterobasal amygdala is connected to the occipital visual cortices [Amaral and Price, 1984; Amaral et al., 1992]. In principle, the bidirectional flow of information between the IOG and amygdala should be beneficial for achieving efficient face processing, because these regions receive visual input via different pathways [Gschwind et al., 2012; Rafal et al., 2015; Tamietto et al., 2012] and conduct different types of computation [Haxby et al., 2000]. To the best of our knowledge, our results represent the first evidence that the IOG and amygdala communicate rapidly with each other during face processing.

Related to our second research question regarding how the IOG and amygdala communicate during face processing, spectral profiles revealed that the inter-regional modulatory effect between the IOG and amygdala during face processing (both upright face vs. upright mosaic and upright face vs. upright house conditions) involved same- and cross-frequency couplings, including gamma-band activity. These results are consistent with those of several previous empirical studies conducted on humans and animals that have reported that same- and cross-frequency couplings involving gamma-band oscillations are evident in inter-regional communication for several different kinds of information processing [e.g., Rodriguez et al., 1999; Friese et al., 2013; for reviews, see von Stein

and Sarnthein, 2000; Varela et al., 2001; Canolty and Knight, 2010]. Furthermore, the present results from the spectral profiles revealed that amygdala–IOG inter-regional modulation for face-inversion effect (upright face superiority effect; upright face vs. inverted face conditions) involved the gamma–gamma same-frequency coupling. Because the inverted presentation of faces specifically impairs the configural/holistic processing of faces [Civile et al., 2014], this finding suggests that the gamma–gamma coupling from the amygdala to the IOG is involved in the configural/holistic processing of faces; other inter-regional couplings related to face effect, such as the IOG–amygdala theta/alpha–gamma and amygdala–IOG gamma–theta/alpha couplings, may be related to featural processing. Taken together, these results suggest that the IOG and amygdala communicate with each other by utilizing the same- and cross-frequency entrainments of gamma-band oscillations during various types of face processing.

What are the information-processing functions of these rapid inter-regional same- and cross-frequency couplings during face processing? Because the IOG and amygdala are thought to be responsive to perceptual and emotional processing, respectively [Haxby et al., 2000], we speculate that the bidirectional communication between these regions implements perceptual–emotional interactions. Consistent with this notion, previous behavioral studies have shown that the perceptual and emotional aspects of faces interact with each other, both in the direction of perception to emotion [McKelvie, 1995; Calder et al., 2000] and that of emotion to perception [Öhman et al., 2001; Milders et al., 2006; Sato and Yoshikawa, 2010]. Furthermore, behavioral studies demonstrated that, relative to other objects, the processing of faces is associated with efficient perception [e.g., Purcell and Stewart, 1986] and robust representation [e.g., Yin, 1969]. Thus, it is possible that these effects may be accounted for, at least in part, by the rapid inter-regional cross- and same-frequency couplings within the IOG–amygdala network. This idea is consistent with the findings of several previous electrophysiological studies that showed that inter-regional cross- and same-frequency couplings are related to effective information processing [e.g., Fries et al., 2013; for reviews, see Hanslmayr and Staudigl, 2014]. However, the relationship between neural oscillatory activity and information processing appears to be inconsistent and somewhat unclear; studies have reported that increases [e.g., Fries et al., 2013] as well as decreases [e.g., Fell et al., 2001] in inter-regional oscillatory couplings are associated with better cognitive performance [for a review, see Hanslmayr and Staudigl, 2014]. Thus, the careful investigation of the information-processing functions of same- and cross-frequency couplings between the IOG and amygdala during face processing is an important matter for future research.

In addition to the common gamma-band-dependent signal transmission across the IOG and amygdala, the spectral profiles in intra- and inter-regional modulatory couplings revealed different patterns across these regions. Specifically, although the IOG showed face-related modulatory effects in the low-frequency (e.g., theta) band, the amygdala did not show such low-frequency modulatory effects. These differences are consistent with the face-related activation patterns in these regions, in which the IOG shows both low- and gamma-band activation in response to faces [Sato et al., 2014], whereas the amygdala shows only gamma-band activation [Sato et al., 2012]. These results suggest that only the neural oscillations that produce strong signals during local computation participate in

intra- and inter-regional communication with other neuronal oscillations during the observation of faces.

Several limitations to this study should be acknowledged. First, we controlled for the mean luminance only and not other visual properties, such as the luminance contrasts and spatial frequency, across stimulus categories. Several scalp-recorded EEG studies have reported that these factors can modulate face-related neural activity, although these factors do not solely account for the differences in such activity in response to faces vs. other objects [e.g., Holmes et al., 2005; Halit et al., 2006; Itier et al., 2006]. To investigate the effects of these visual factors on communication between the IOG and amygdala during face processing, further studies that use other types of control stimuli are needed.

Second, we analyzed spectral profiles using thresholds that were uncorrected for multiple comparisons, and thus the results should be interpreted as descriptive. We conducted exploratory analyses to provide more information [Rothman, 1990] in this first investigation of the electric communication between the IOG and amygdala. The generation and testing of hypotheses based on the present findings would be warranted in future research.

Third, we analyzed amplitude–amplitude couplings to depict intra- and inter-regional functional couplings, because this analysis was the only option available within the framework of DCM [cf. Chen et al., 2008]. However, several different types of same- and cross-frequency couplings have been proposed, such as phase–phase and phase–amplitude couplings. It remains unclear how these different types of couplings are related to each other and what types of intra- and inter-regional couplings play important roles in the processing of information [cf. Canolty and Knight, 2010]. Future studies that analyze different types of couplings between the IOG and amygdala during face processing would be beneficial to achieve a deeper understanding of communication between these regions.

Finally, because the locations of the electrode implantation were chosen based solely on clinical criteria, it was not possible to investigate other brain regions related to face processing. It is highly plausible that the IOG and amygdala send signals to other brain regions. The effective connectivity between these regions could also be mediated through other omitted regions [cf. Friston, 2011], such as the fusiform gyrus (FG). Several previous functional neuroimaging studies have reported that the FG is active during the observation of faces [e.g., Sergent et al., 1992; Haxby et al., 1994; for a review, see Kanwisher and Yovel, 2006]. Intracranial EEG [Engell and McCarthy, 2011; Klopp et al., 1999; Lachaux et al., 2005] and MEG [Uono et al., 2017] studies reported that this region exhibits gamma-band activation in response to faces. However, the manner in which the FG may contribute to the functional network that includes the IOG and amygdala remains unknown. Whereas some neuroimaging studies have shown that the FG receives face-related signals from the IOG [e.g., Fairhall and Ishai, 2007], other studies have demonstrated that it conducts face processing independently of the IOG [e.g., Rossion et al., 2011]. Similarly, although some neuroimaging studies reported that the amygdala modulates activity in widespread cortical regions, including the FG, during the processing of facial stimuli [e.g., Furl et al., 2013; Sato et al., 2017], other studies failed to detect this type of amygdala–FG modulation [e.g., Goulden et al., 2012]. A previous MEG study that

investigated the effective connectivity between the IOG and FG during face processing reported positive same-frequency theta/alpha/beta couplings and negative cross-frequency theta–beta couplings from the IOG to the FG [Furl et al., 2014]; however, this study did not investigate amygdala activity and high (> 48 Hz) frequency ranges. To clarify these issues and further elucidate the electrical communication among the brain regions involved in face processing, electrophysiological studies that evaluate the FG in conjunction with the IOG and amygdala should be conducted.

In summary, our DCM for induced responses to human intracranial EEG data revealed face-specific bidirectional modulatory interactions between the IOG and amygdala regarding comparisons of upright face vs. upright mosaic, upright face vs. upright house, and upright face vs. inverted face conditions. In addition, spectral profiles of the modulatory effects revealed cross- (e.g., theta–gamma) and same- (e.g., gamma–gamma) frequency couplings. These results suggest that the IOG and amygdala rapidly communicate with each other, using various types of oscillations to efficiently process faces.

ACKNOWLEDGMENTS

This study was supported by funds from the Benesse Corporation, the JSPS Funding Program for Next Generation World-Leading Researchers (LZ008), and the JSPS KAKENHI (15K04185). The authors declare no competing financial or other interests.

REFERENCES

- Adrian ED (1942): Olfactory reactions in the brain of the hedgehog. *J Physiol* 100:459–473.
- Allison T, Puce A, Spencer DD, McCarthy G (1999): Electrophysiological studies of human face perception. I: Potentials generated in occipitotemporal cortex by face and non-face stimuli. *Cereb Cortex* 9:415–430.
- Amaral DG, Price JL (1984): Amygdalo-cortical projections in the monkey (*Macaca fascicularis*). *J Comp Neurol* 230: 465–496.
- Amaral DG, Price JL, Pitkanen A, Carmichael ST (1992): Anatomical organization of the primate amygdaloid complex. In: Aggleton JP, editor. *The amygdala: Neurobiological aspects of emotion, memory, and mental dysfunction*. New York: Wiley-Liss. p 1–66.
- Amunts K, Kedo O, Kindler M, Pieperhoff P, Mohlberg H, Shah NJ, Habel U, Schneider F, Zilles K (2005): Cytoarchitectonic mapping of the human amygdala, hippocampal region and entorhinal cortex: Intersubject variability and probability maps. *Anat Embryol* 210: 343–352.
- Blonder LX, Smith CD, Davis CE, Kesler-West ML, Garrity TF, Avison MJ, et al. (2004): Regional brain response to faces of humans and dogs. *Brain Res Cogn Brain Res* 20:384–394.

- Bruce V, Young AW (1986): Understanding face recognition. *Br J Psychol* 77:305–327.
- Calder AJ, Young AW, Keane J, Dean M (2000): Configural information in facial expression perception. *J Exp Psychol Hum Percept Perform* 26:527–551.
- Canolty RT, Edwards E, Dalal SS, Soltani M, Nagarajan SS, Kirsch HE, Berger MS, Barbaro NM, Knight RT (2006): High gamma power is phase-locked to theta oscillations in human neocortex. *Science* 313:1626–1628.
- Canolty RT, Knight RT (2010): The functional role of cross-frequency coupling. *Trends Cogn Sci* 14:506–515.
- Catani M, Jones DK, Donato R, Ffytche DH (2003): Occipito-temporal connections in the human brain. *Brain* 126:2093–2107.
- Chen CC, Kiebel SJ, Friston KJ (2008): Dynamic causal modelling of induced responses. *Neuroimage* 41:1293–1312.
- Chen CC, Henson RN, Stephan KE, Kilner JM, Friston KJ (2009): Forward and backward connections in the brain: A DCM study of functional asymmetries. *Neuroimage* 45:453–462.
- Chen CC, Kiebel SJ, Kilner JM, Ward NS, Stephan KE, Wang WJ, Friston KJ (2012): A dynamic causal model for evoked and induced responses. *Neuroimage* 59:340–348.
- Civile, C, McLaren RP, McLaren IP (2014): The face inversion effect-Parts and wholes: Individual features and their configuration. *Q J Exp Psychol* 67:728–746.
- Davies-Thompson J, Andrews TJ (2012): Intra- and interhemispheric connectivity between face-selective regions in the human brain. *J Neurophysiol* 108:3087–3095.
- Eickhoff SB, Stephan KE, Mohlberg H, Grefkes C, Fink GR, Amunts K, Zilles K (2005): A new SPM toolbox for combining probabilistic cytoarchitectonic maps and functional imaging data. *Neuroimage* 25: 1325–1335.
- Ekman P, Friesen WV. (1975). *Unmasking the face: A guide to recognizing emotions from facial clues*. New Jersey: Prentice-Hall.
- Engell AD, McCarthy G (2011): The relationship of gamma oscillations and face-specific ERPs recorded subdurally from occipitotemporal cortex. *Cereb Cortex* 21:1213–1221.
- Fairhall SL, Ishai A (2007): Effective connectivity within the distributed cortical network for face perception. *Cereb Cortex* 17:2400–2406.
- Farah MJ, Tanaka JW, Drain HM (1995): What causes the face inversion effect? *J Exp Psychol Hum Percept Perform* 21:628–634.

- Fell J, Klaver P, Lehnertz K, Grunwald T, Schaller C, Elger CE, Fernandez G (2001): Human memory formation is accompanied by rhinal-hippocampal coupling and decoupling. *Nat Neurosci* 4:1259–1264.
- Foucher JR, Otzenberger H, Gounot D (2003): The BOLD response and the gamma oscillations respond differently than evoked potentials: an interleaved EEG-fMRI study. *BMC Neurosci* 4:22.
- Friese U, Köster M, Hassler U, Martens U, Trujillo-Barreto N, Gruber T (2013): Successful memory encoding is associated with increased cross-frequency coupling between frontal theta and posterior gamma oscillations in human scalp-recorded EEG. *Neuroimage* 66:642–647.
- Friston K (2011): Dynamic causal modeling and Granger causality Comments on: The identification of interacting networks in the brain using fMRI: Model selection, causality and deconvolution. *NeuroImage* 58:303–305.
- Friston KJ, Harrison L, Penny W (2003): Dynamic causal modelling. *Neuroimage* 19:1273–1302.
- Furl N, Coppola R, Averbeck BB, Weinberger DR (2014): Cross-frequency power coupling between hierarchically organized face-selective areas. *Cereb Cortex* 24:2409–2420.
- Furl N, Henson RN, Friston KJ, Calder AJ (2013): Top-down control of visual responses to fear by the amygdala. *J Neurosci* 33:17435–17443.
- Furl N, Henson RN, Friston KJ, Calder AJ (2015): Network interactions explain sensitivity to dynamic faces in the superior temporal sulcus. *Cereb Cortex* 25:2876–2882.
- Gauthier I, Skudlarski P, Gore JC, Anderson AW (2000): Expertise for cars and birds recruits brain areas involved in face recognition. *Nat Neurosci* 3 :191–197.
- Gothard KM, Battaglia FP, Erickson CA, Spitler KM, Amaral DG (2007): Neural responses to facial expression and face identity in the monkey amygdala. *J Neurophysiol* 97:1671–1683.
- Goulden N, McKie S, Thomas EJ, Downey D, Juhasz G, Williams SR, Rowe JB, Deakin JF, Anderson IM, Elliott R (2012): Reversed frontotemporal connectivity during emotional face processing in remitted depression. *Biol Psychiatry* 72:604–611.
- Gschwind M, Pourtois G, Schwartz S, Van De Ville D, Vuilleumier P (2012): White-matter connectivity between face-responsive regions in the human brain. *Cereb Cortex* 22:1564–1576.
- Halit H, de Haan M, Schyns PG, Johnson MH (2006): Is high-spatial frequency information used in the early stages of face detection? *Brain Res* 1117: 154–161.
- Hanslmayr S, Staudigl T (2014): How brain oscillations form memories--a processing based perspective on oscillatory subsequent memory effects. *Neuroimage* 85:648–655.
- Haxby JV, Hoffman EA, Gobbini MI (2000): The distributed human neural system for face perception. *Trends Cogn Sci* 4:223–33.

- Haxby JV, Horwitz B, Ungerleider LG, Maisog JM, Pietrini P, Grady CL (1994): The functional organization of human extrastriate cortex: a PET-rCBF study of selective attention to faces and locations. *J Neurosci* 14: 6336–6353.
- Herrmann CS, Frund I, Lenz D (2010): Human gamma-band activity: A review on cognitive and behavioral correlates and network models. *Neurosci Biobehav Rev* 34:981–992.
- Hershler O, Hochstein S (2005): At first sight: A high-level pop out effect for faces. *Vision Res* 45:1707–1724.
- Holmes A, Winston JS, Eimer M (2005): The role of spatial frequency information for ERP components sensitive to faces and emotional facial expression. *Brain Res Cogn Brain Res* 25: 508–520.
- Hurlemann R, Rehme AK, Diessel M, Kukulja J, Maier W, Walter H, Walter H, Cohen MX (2008): Segregating intra-amygdalar responses to dynamic facial emotion with cytoarchitectonic maximum probability maps. *J Neurosci Methods* 172:13–20.
- Ishai A, Schmidt CF, Boesiger P (2005): Face perception is mediated by a distributed cortical network. *Brain Res Bull* 6:87–93.
- Itier RJ, Latinus M, Taylor MJ (2006): Face, eye and object early processing: what is the face specificity? *Neuroimage* 29: 667–676.
- Jonas J, Descoins M, Koessler L, Colnat-Coulbois S, Sauvée M, Guye M, Vignal JP, Vespignani H, Rossion B, Maillard L (2012): Focal electrical intracerebral stimulation of a face-sensitive area causes transient prosopagnosia. *Neuroscience* 22:281–288.
- Kanwisher N, Yovel G (2006): The fusiform face area: A cortical region specialized for the perception of faces. *Philos Trans R Soc Lond Biol* 361: 2109–2128.
- Klopp J, Halgren E, Marinkovic K, Nenov V (1999): Face-selective spectral changes in the human fusiform gyrus. *Clin Neurophysiol* 110:676–682.
- Lachaux JP, George N, Tallon-Baudry C, Martinerie J, Hugueville L, Minotti L, Kahane P, Renault B (2005): The many faces of the gamma band response to complex visual stimuli. *Neuroimage* 25:491–501.
- Lachaux JP, Rudrauf D, Kahane P (2003): Intracranial EEG and human brain mapping. *J Physiol Paris* 97:613–628.
- Landau AN, Bentin S (2008): Attentional and perceptual factors affecting the attentional blink for faces and objects. *J Exp Psychol Hum Percept Perform* 34:818–830.
- Latini F (2015): New insights in the limbic modulation of visual inputs: the role of the inferior longitudinal fasciculus and the Li-Am bundle. *Neurosurg Rev* 38:179–189.

- Liebe S, Hoerzer GM, Logothetis NK, Rainer G (2012): Theta coupling between V4 and prefrontal cortex predicts visual short-term memory performance. *Nat Neurosci* 15:456–462.
- Lisman JE, Jensen O (2013): The theta-gamma neural code. *Neuron* 77:1002–1016.
- Litvak V, Mattout J, Kiebel S, Phillips C, Henson R, Kilner J, Barnes G, Oostenveld R, Daunizeau J, Flandin G, Penny W, Friston K (2011): EEG and MEG data analysis in SPM8. *Comput Intell Neurosci* 2011:852961.
- Liu J, Harris A, Kanwisher N (2010a): Perception of face parts and face configurations: An fMRI study. *J Cogn Neurosci* 22:203–211.
- Liu L, Vira A, Friedman E, Minas J, Bolger D, Bitan T, Booth J (2010b): Children with reading disability show brain differences in effective connectivity for visual, but not auditory word comprehension. *PLoS One* 5:e13492.
- Logothetis NK, Pauls J, Augath M, Trinath T, Oeltermann A (2001): Neurophysiological investigation of the basis of the fMRI signal. *Nature* 412:150–157.
- McKelvie SJ (1995): Emotional expression in upside-down faces: Evidence for configurational and componential processing. *Br J Soc Psychol* 34:325–334.
- Mihara T, Baba K (2001): Combined use of subdural and depth electrodes. In: Luders HO, Comair YG editors. *Epilepsy Surgery* (second ed.). Philadelphia: Lippincott Williams and Wilkins. p 613–621.
- Milders M, Sahraie A, Logan S, Donnellon N (2006): Awareness of faces is modulated by their emotional meaning. *Emotion* 6:10–17.
- Montgomery SM, Buzsaki G (2007): Gamma oscillations dynamically couple hippocampal CA3 and CA1 regions during memory task performance. *Proc Natl Acad Sci U S A* 104:14495–14500.
- Mukamel R, Fried I (2012): Human intracranial recordings and cognitive neuroscience. *Annu Rev Psychol* 63:511–537.
- Nakamura K, Mikami A, Kubota K (1992): Activity of single neurons in the monkey amygdala during performance of a visual discrimination task. *J Neurophysiol* 67:1447–1463.
- Öhman A, Lundqvist D, Esteves F (2001): The face in the crowd revisited: A threat advantage with schematic stimuli. *J Pers Soc Psychol* 80:381–396.
- Oldfield RC (1971): The assessment and analysis of handedness: the Edinburgh inventory. *Neuropsychologia* 9:97–113.
- Purcell DG, Stewart AL (1986): The face-detection effect. *Bull Psychon Soc* 24:118–120.

- Rafal RD, Koller K, Bultitude JH, Mullins P, Ward R, Mitchell AS, Bell AH (2015): Connectivity between the superior colliculus and the amygdala in humans and macaque monkeys: Virtual dissection with probabilistic DTI tractography. *J Neurophysiol* 114:1947–1962.
- Ro T, Russell C, Lavie N (2001): Changing faces: a detection advantage in the flicker paradigm. *Psychol Sci* 12:94–99.
- Rodriguez E, George N, Lachaux JP, Martinerie J, Renault B, Varela FJ (1999): Perception's shadow: Long-distance synchronization of human brain activity. *Nature* 397:430–433.
- Rosburg T, Ludowig E, Dümpelmann M, Alba-Ferrara L, Urbach H, Elger CE (2010): The effect of face inversion on intracranial and scalp recordings of event-related potentials. *Psychophysiology* 47:147–157.
- Rossion B, Dricot L, Goebel R, Busigny T (2011): Holistic face categorization in higher order visual areas of the normal and prosopagnosic brain: Toward a non-hierarchical view of face perception. *Front Hum Neurosci* 4:225.
- Rossion B, Hanseeuw B, Dricot L (2012): Defining face perception areas in the human brain: A large-scale factorial fMRI face localizer analysis. *Brain Cogn* 79:138–157.
- Rothman KJ (1990): No adjustments are needed for multiple comparisons. *Epidemiology* 1:43–46.
- Sato W, Kochiyama T, Kubota Y, Uono S, Sawada R, Yoshimura S, Toichi M (2016): The association between perceived social support and amygdala structure. *Neuropsychologia* 85:237–244.
- Sato W, Kochiyama T, Uono S, Matsuda K, Usui K, Inoue Y, Toichi M (2012): Temporal profile of amygdala gamma oscillations in response to faces. *J Cogn Neurosci* 24:1420–1433.
- Sato W, Kochiyama T, Uono S, Matsuda K, Usui K, Inoue Y, Toichi M (2014): Rapid, high-frequency, and theta-coupled gamma oscillations in the inferior occipital gyrus during face processing. *Cortex* 60:52–68.
- Sato W, Kochiyama T, Uono S, Yoshikawa S, Toichi M (2017): Direction of amygdala–neocortex interaction during dynamic facial expression processing. *Cereb Cortex* 27:1878–1890.
- Sato W, Yoshikawa S (2010): Detection of emotional facial expressions and anti-expressions. *Vis cogn* 18:369–388.
- Sato W, Yoshikawa S (2013): Recognition memory for faces and scenes. *J Gen Psychol* 140:1–15.
- Sato W, Yoshikawa S, Kochiyama T, Matsumura M (2004): The amygdala processes the emotional significance of facial expressions: An fMRI investigation using the interaction between expression and face direction. *Neuroimage* 22:1006–1013.

- Seghier ML, Josse G, Leff AP, Price CJ (2011): Lateralization is predicted by reduced coupling from the left to right prefrontal cortex during semantic decisions on written words. *Cereb Cortex* 21:1519–1531.
- Sergent J (1984) An investigation into component and configural processes underlying face perception. *Br J Psychol* 75 221–242.
- Sergent J, Ohta S, MacDonald B (1992): Functional neuroanatomy of face and object processing. A positron emission tomography study. *Brain* 115:15–36.
- Stephan KE, Penny WD, Daunizeau J, Moran RJ, Friston KJ (2009): Bayesian model selection for group studies. *Neuroimage* 46:1004–1017.
- Tallon-Baudry C, Bertrand O, Delpuech C, Pernier J (1996): Stimulus specificity of phase-locked and non-phase-locked 40 Hz visual responses in human. *J Neurosci* 16:4240–4249.
- Tanaka JW, Farah MJ (1993): Parts and wholes in face recognition. *Q J Exp Psychol A* 46: 225–245.
- Tanaka JW, Simonyi D (2016): The "parts and wholes" of face recognition: A review of the literature. *Q J Exp Psychol* 69:1876–1889.
- Tamietto M, Pullens P, de Gelderm B, Weiskrantz L, Goebel R (2012): Subcortical connections to human amygdala and changes following destruction of the visual cortex. *Curr Biol* 22:1449–1455.
- Tottenham N, Leon AC, Casey BJ (2006): The face behind the mask: A developmental study. *Dev Sci* 9:288–294.
- Uono S, Sato W, Kochiyama T, Kubota Y, Sawada R, Yoshimura S, Toichi M (2017): Time course of gamma-band oscillation associated with face processing in the inferior occipital gyrus and fusiform gyrus: A combined fMRI and MEG study. *Hum Brain Mapp* 38:2067–2079.
- Varela F, Lachaux JP, Rodriguez E, Martinerie J (2001): The brainweb: Phase synchronization and large-scale integration. *Nat Rev Neuroscience*, 2:229–239.
- von Stein A, Sarnthein J (2000): Different frequencies for different scales of cortical integration: From local gamma to long range alpha/theta synchronization. *Int J Psychophysiol* 38:301–313.
- Yin RK (1969): Looking at upside-down faces. *J Exp Psychol* 81:141–145.
- Yin RK (1970): Face recognition by brain-injured patients: a dissociable ability? *Neuropsychologia* 8:395–402.
- Young AW, Hellawell D, Hay DC (1987): Configurational information in face perception. *Perception* 16:747–759.

Table 1. Demographic and clinical information of patients.

ID	Sex	Age	Handedness	IQ	Epileptic focus	Comorbidity	Medication
S1	Female	43	Right	79	Left hippocampus	None	CBZ (100mg); CLB (5mg)
S2	Male	22	Right	118	Right temporal cortex	None	CBZ (400 mg); CLB (10mg)
S3	Female	35	Right	63	Left hippocampus	None	CBZ (400 mg); CLB (10mg)
S4	Female	33	Right	104	Right hippocampus	None	PHT (250mg)
S5	Female	31	Right	91	Right hippocampus	None	CBZ (400 mg); CZP (1mg)
S6	Female	43	Right	96	Right hippocampus	None	CBZ (600 mg); CLB (5mg)

IQ = The full-scale intelligence quotient measured using the revised Wechsler Adult Intelligence Scale.

CBZ = Carbamazepin; CLB = Clobazam; PHT = Phenytoin; CZP = Clonazepam.

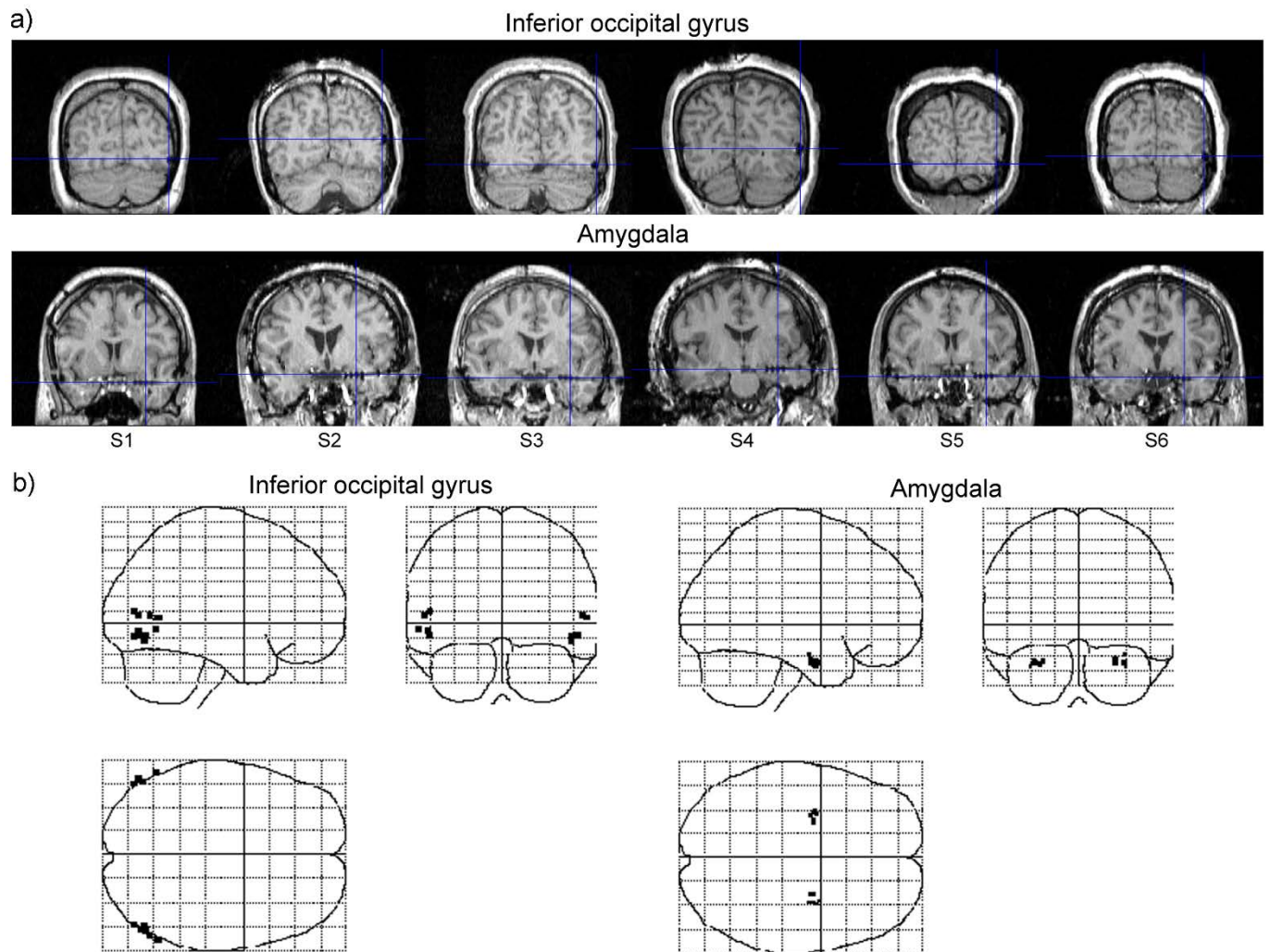


Figure 1.

(a) Anatomical magnetic resonance images of participants. Blue crosshairs indicate electrode locations in the inferior occipital gyrus and amygdala in the right hemispheres. Numbers with the prefix “S” indicate the participants’ identifications. (b) Glass brain projections of the electrode coordinates (black points) in the Montreal Neurological Institute space.

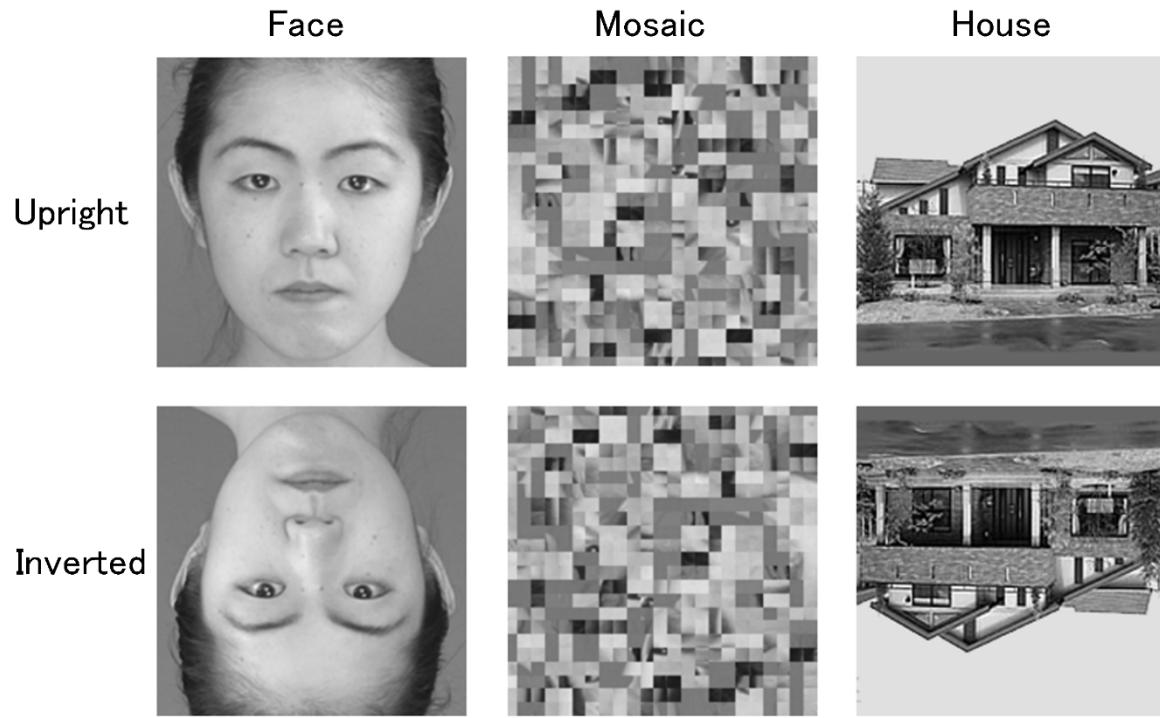


Figure 2.

Examples of stimulus presentations.

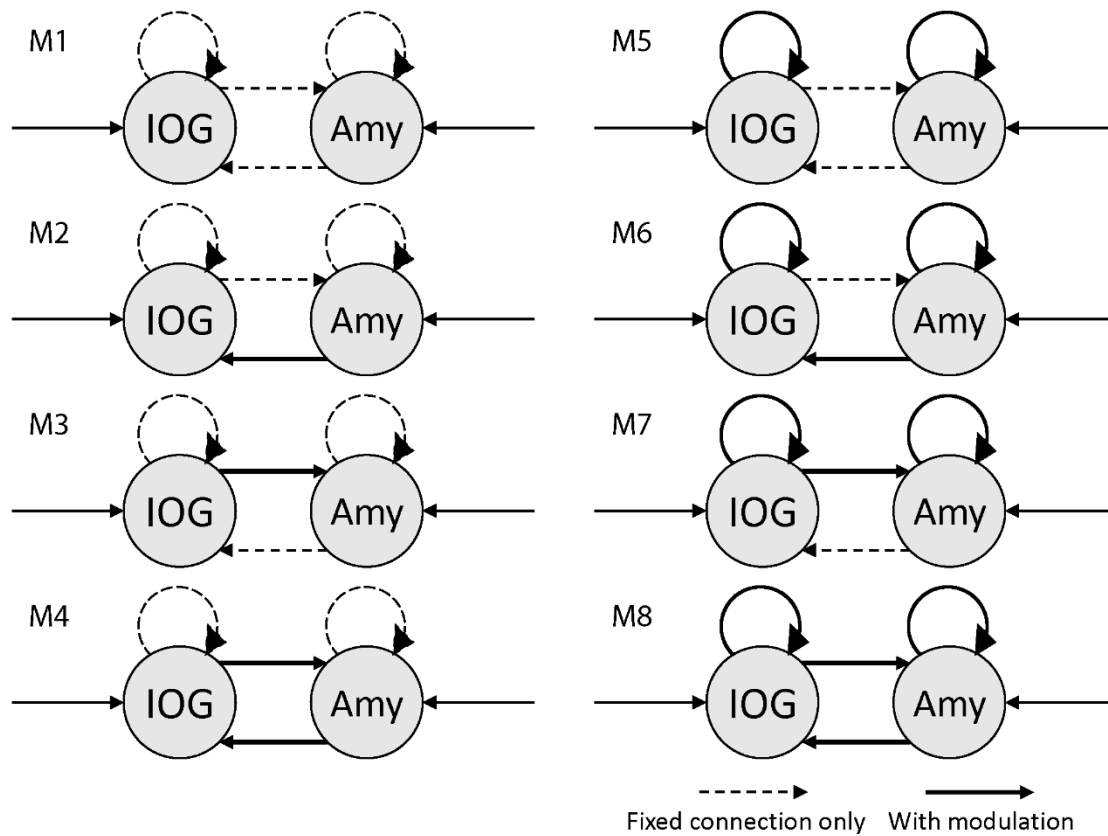


Figure 3.

Analyzed models. Arrows indicate driving inputs to and intrinsic connections between the inferior occipital gyrus (IOG) and amygdala (Amy). Thick lines indicate the locations of the modulatory effects of face or face inversion. Dashed lines indicate intrinsic connections without a modulatory effect. Candidates included models with modulatory effects on no connections (M1), on inter-regional connections alone (M2–4), on intra-regional connections alone (M5), and on both inter-regional and intra-regional connections (M6–8); models with unidirectional (M2–3 and M6–7) and bidirectional inter-regional connections (M4 and M8).

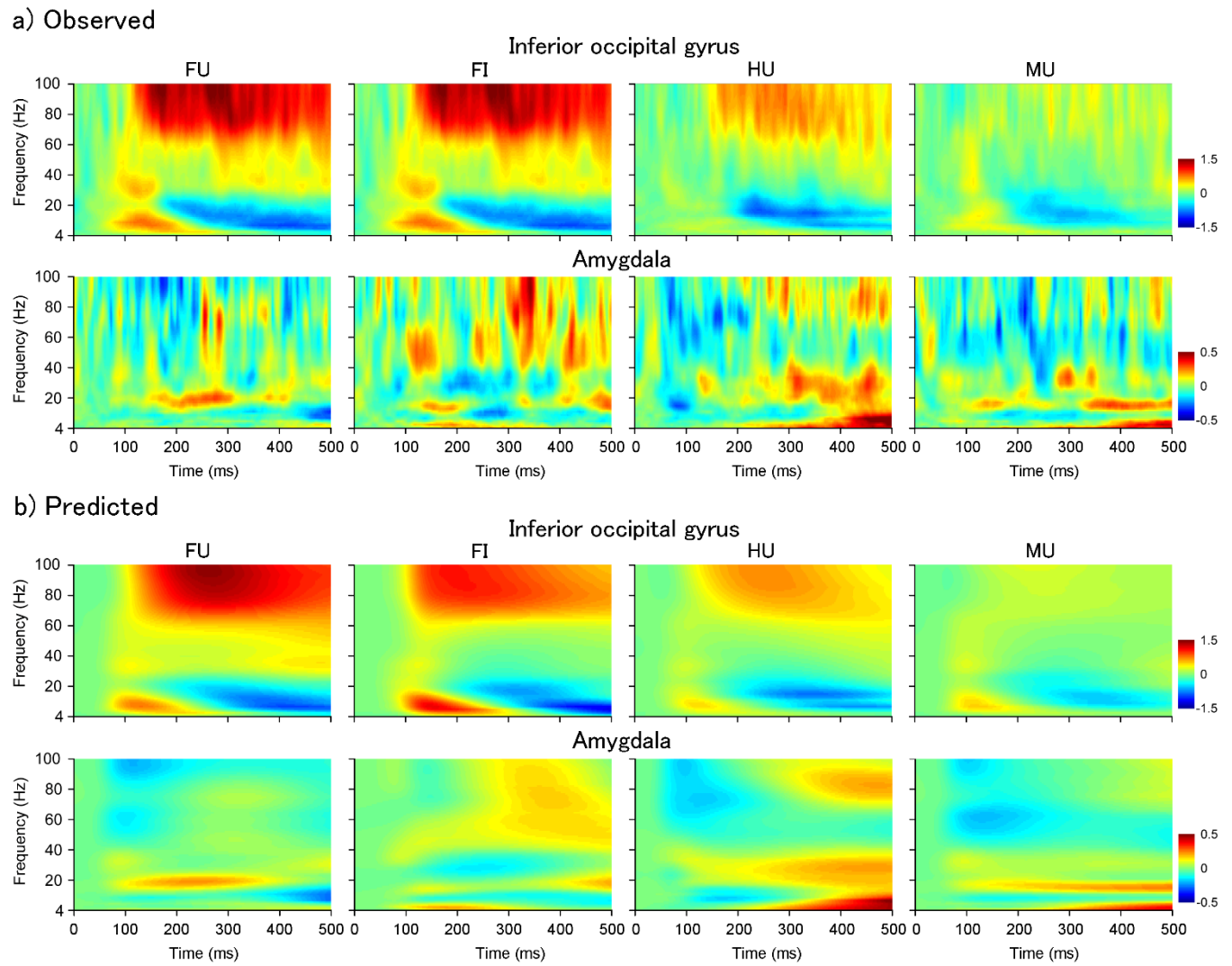
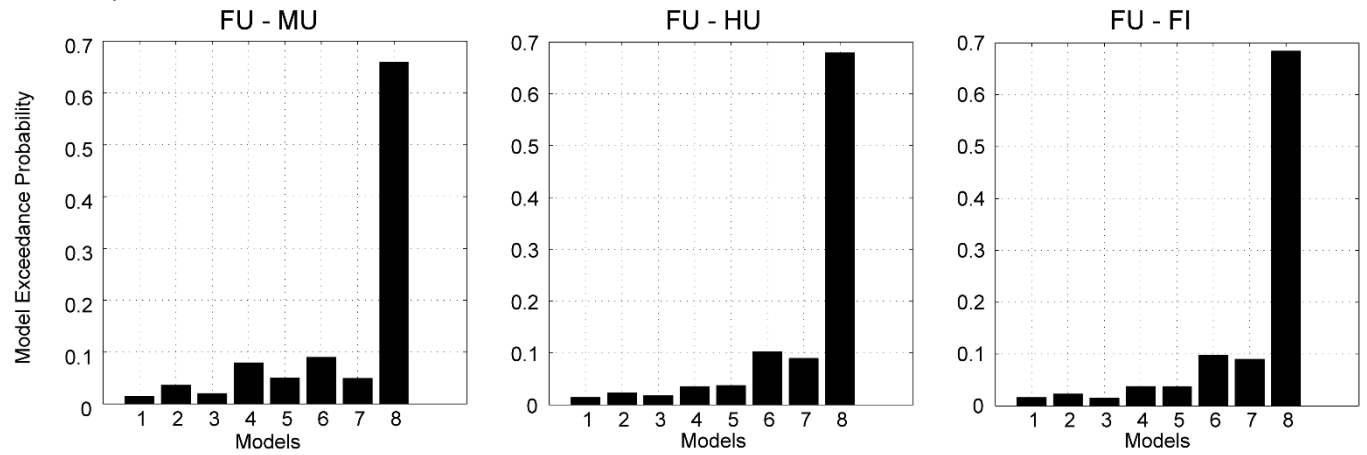


Figure 4.

Observed (a) and predicted (b) time–frequency responses of the right inferior occipital gyrus (upper) and the right amygdala (lower) averaged across all participants. The predicted responses were generated from the winning model (M8 in Fig. 2). FU = upright face; FI = inverted face; HU = upright house; MU = upright mosaic.

a) Group



b) Individual

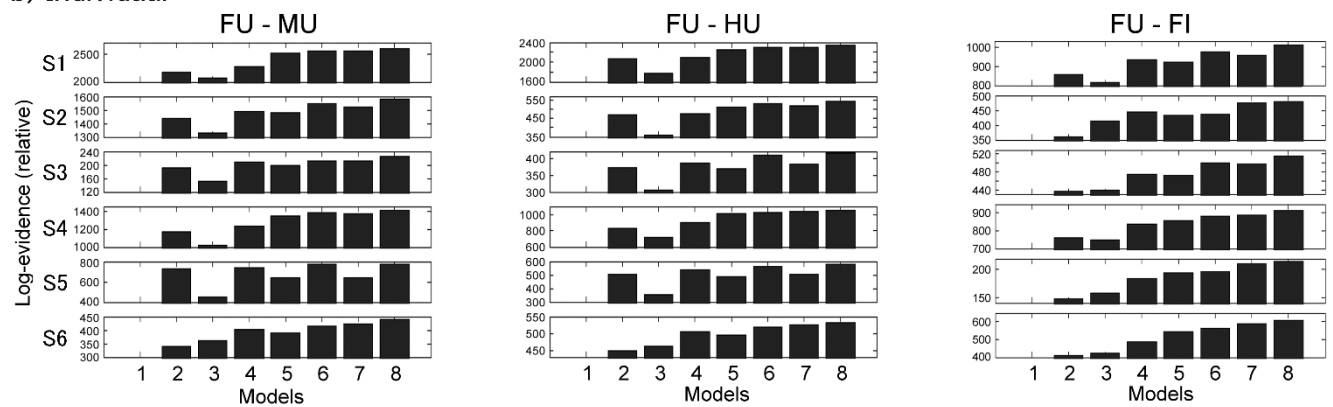


Figure 5.

(a) Exceedance probabilities of models for the face effect based on upright face (FU) vs. upright mosaic (MU), FU vs. upright house (HU), and FU vs. inverted face (FI) in the Bayesian model selection in group analyses. (b) Exceedance probabilities of models for the face effect based on FU versus MU, FU versus HU, and FU versus FI in the Bayesian model selection in individual analyses. Numbers with the prefix “S” indicate the participants’ identifications.

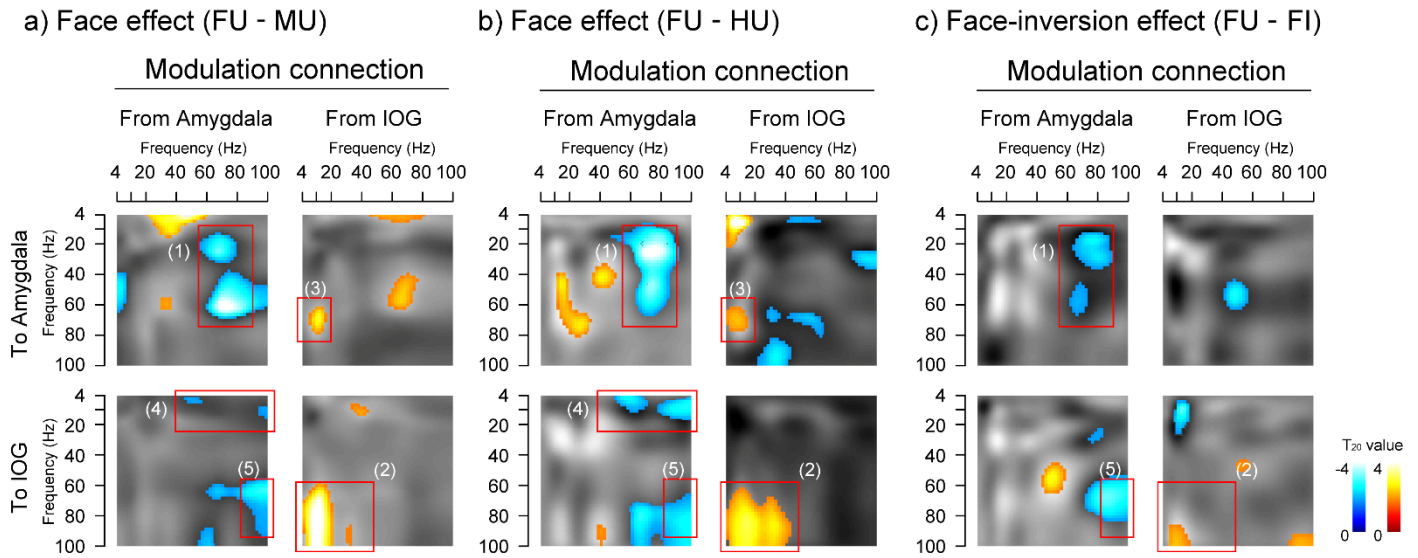


Figure 6.

The spectral profiles of modulatory couplings based on comparisons of upright face (FU) vs. upright mosaic (MU) (a), FU vs. upright house (HU) (b), and FU vs. inverted face (FI) (c). Intra-regional (from the amygdala to the amygdala and from the inferior occipital gyrus (IOG) to the IOG) and inter-regional (from the IOG to the amygdala and from the amygdala to the IOG) couplings are shown for each effect. SPM{t} values for significant positive/excitatory (red–yellow blobs) and negative/inhibitory (blue–cyan blobs) effects are overlaid on the corresponding grayscale contrast image. Red boxes indicate clusters of consistent same- and cross-frequency couplings across both face effect contrasts ((a) and (b)).